Egypt. J. Chem. **Vol. 63**, No. 10 pp. 4005 - 4016 (2020)

Egyptian Journal of Chemistry

http://ejchem.journals.ekb.eg/

Synthesis, characterization and cytotoxic activity study of Cu (II), Co (II), Mn (II), Ni (II) and Cr (III) Metal Complexes with new guanidine Schiff base against the hepatocellular Carcinoma (HCAM) cancer cell

Sara K. Yassin, Jasim M. S. Alshawi,* Zainab A. M. Salih

Chemistry Department, College of Education for Pure Sciences, Basrah University, Basrah, Iraq

Abstract

In this research, a new guanidine ligand was synthesized from the condensation reaction of 1,2-hydrazinedicarboximidamide and indol-3-carboxaldehyde and its derived metal transition complexes of Co (II), Ni (II), Mn (II), Cu (II) and Cr (III) have been synthesized by reaction of metal chlorides with guanidine ligand in the molar ratio 2:1 (M: L). The guanidine ligand and its metal complexes were characterized by different spectroscopic and analytical techniques, these studies result suggests that the metal complexes have tetrahedral geometry. The cytotoxic activity of the guanidine Schiff base and its metal complexes were studied on hepatoma cellular carcinoma (HCAM) cell line.

Keywords: Guanidine-indole; Thioureas; Complexes; MTT assay

Introduction

Guanidine and its derivatives can be seen in many natural compounds that have a significant area of biological activities such as anti-inflammatory, anti-diabetic, anti-clotting agents, exhibit cytotoxic, antiviral, antibacterial, and anti-parasitic [1, 2]. Guanidine is an important class of compounds in organic and biochemistry that possesses the formula $HN=C(NH_2)_2$, where the carbon atom is bonded to three nitrogen atoms. Which is among the strongest known organic bases and it has very weak pKa that are difficult to accurately measure in water . There are several approaches for the synthesis of guanidine from different materials and reagents, one of these approaches is the diversion of thioureas to guanidine in the presence of a coupling reagent. Their conversion to guanidine regularly needs initial activation [3]. A number of reviewed articles had been reported on Schiff base compounds derived from guanidine are of prominence in organic synthesis, as they are used as intermediates to prepare a number of organic compounds [4-7]. Some Schiff base derivatives were prepared by the interaction of aminoguanidine with the different substituted benzaldehyde [8, 9], as these compounds proved to possess anti-bacterial and anti-cancer activities [10]. Also, various aminoguanidine derivatives exhibit anti-tumor activity by forming metal ion complexes [11, 12]. Three complexes of copper (II) were synthesized from 2-aminobenzimidazole and o-vanillin as primary ligand and N, N-donor heterocyclic bases (1,10-phenanthroline and 2,2′-bipyridyl) as co-ligand are the examples containing guanidine Schiff base ligand, and these complexes considered to have a first vision on their potential anti-cancer activity against MCF-7 (human breast cancer)cell lines as well as anti-inflammatory, antipyretic and analgesic activities [13].

In this paper, five new guanidine-indole complexes were synthesized from the Schiff base reaction of

*Corresponding author e-mail: jasim.salih@uobasrah.edu.iq.
Receive Date: 03 August 2020, Revise Date: 21 September 2020, Accept Date: 10 October 2020
DOI: 10.21608/EJCHEM.2020.37893.2778

1,2-hydrazinedicarboximidamide with indol-3-carboxaldehyde. All complexes have a tetra-coordinated metal centre, binding two donors of the corresponding Schiff base guanidine ligand *via* the imine nitrogen atom and two nitrogen atoms of the indole unit. This motivates us to study the biological activity of guanidine ligand and its complexes against hepatoma cellular carcinoma (HACM) cell line.

Experimental

Materials and Methods

Aldrich and Merck obtained all the reagents and solvents and used them without further purification. Infrared spectra were collected using KBr pellets on FTIR-84005-SHIMADZU. Melting points were obtained using Thermo-scientific apparatus. Ligand spectrum ^{1}H and ^{13}C-NMR was obtained on Bruker-400HZ and recorded at room temperature in DMSO. UV-Visible spectra on uv-win5 were reported using 10mm quartz cells. Mass spectra were run at70 eV with Agilent technologies. The complexes molar conductance of 10^{-3} M solutions in DMF were measured at 25°C using Wissenschaftlich-Technische Werkstätten GmbHin 82362 Weilhaimapparatus. Magnetic properties on Auto magnetic susceptibility balance were reported using glass tubes with a diameter of 0.324 cm. Thin layer chromatography (TLC) has tracked the completion of reactions.

Synthesis of the Guanidine ligand and its metal complexes

General synthetic route of the guanidine ligand, (L)

The ligand L ($C_{38}H_{28}N_{10}$) was prepared from the reaction of thiourea (24.57 g, 0.3228 mol) and hydrazine hydrate (8 g, 0.0689 mol) in dry ethanol (100 ml), before the mixture was subjected to heating for a period 3 hours with stirring. Cool the reaction mixture at room temperature and the resulting precipitate was then filtered and cleansed through recrystallization from ethanol to isolated the 1,2-hydrazinedicarboximidamide product [14]. Indol-3-carboxaldehyde (5.8 g, 0.039 mol) in dry ethanol (25ml) and glacial acetic acid (2-3) drops was added. This combination was stirred about ten minutes, the solution of the 1,2-hydrazinedicarboximidamide (1.12 g, 0.0096 mol) in dry ethanol (15ml) was then added gradually and the reaction mixture was refluxed with stirring for six hours, the yellow precipitate was retrieved through filtration, rinsed by ethanol several times and then allowed to dry. Ultimately, the target product was acquired through there crystallization from ethanol (Scheme 1). Yellow colour; yield: 75 %; M.P 255-258 °C; FTIR (ν cm^{-1}): 3107 (ν N-H), 3059 (ν CH aromatic),1672 (ν C=N), 1516-1440 (ν C=C), 1365 (ν C-N), 1132(ν N-N); ^{1}H NMR (DMSO, 400 MHz; δ ppm) δ: 11.51 (s, 2H, 2NH), 8.92 (s, 2H, 2CH =N), 7.14-8.40 (m, 10H, Ar-H); ^{13}C NMR (DMSO, 400 MHz; δ ppm): 111.7, 111.9, 112.1, 112.4, 120.3, 120.5, 122.1, 122.4, 122.6, 122.8, 124.2, 124.7, 129.5, 131.8, 137.0, 137.2 (aromatic carbons), 155.11 (-C=N-N), 185.01 (CH=N); MS: m/z: 624[M^+], 118[M^+], 146[M^+], 341[M^+] ; UV-vis. in DMSO, cm^{-1} (transition): 279 (π→π*) and 357 (n→π*).

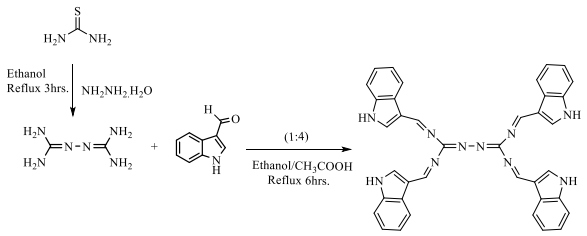

Scheme 1. Synthesis of guanidine ligand (L).

Synthesis of transition metal complexes (1–5)

The guanidine L($C_{38}H_{28}N_{10}$) (0.156g,1mmol) in (2:4:4 ml) of (DMF: EtOH: MeOH) respectively was mixed with metal chlorides (2mmol) of $CuCl_2.2H_2O$, $CoCl_2.6H_2O$, $MnCl_2.4H_2O$, $NiCl_2.6H_2O$ and $CrCl_3.6H_2O$. This reaction mixture was carried out by heating under reflux with stirring for three hours, through filtration the precipitate was separated from the reaction. The precipitate was washed with diethyl ether and dried in a desiccator over activated silica gel [15] (Fig.1).

Complex 1.

Pale brown colour; yield: 59 %; M.P>300 °C; FTIR (ν cm^{-1}):1637 (ν C=N), 1521 (ν C=C), 1444 (ν C-N), 1122(ν N-N), 640(νM-N) and 486 (νM-NH); UV-vis. in DMSO, cm^{-1} (transition):262, 296 (π→π*), 336 (n→π*) and 342 (d-d); MS: m/z: 750[M^+];Λ_m(ohm^{-1} cm^2 mol^{-1}) 77.6; μeff (BM) 1.75.

Complex 2.

Green colour; yield: 66 %; M.P>300 °C; FTIR (ν cm^{-1}): 1635 (ν C=N), 1562 (ν C=C), 1446 (ν C-N), 1131 (ν N-N), 532(νM-N) and 430 (νM-NH); UV-vis. in DMSO, cm^{-1} (transition): 261, 298 ($\pi\rightarrow\pi^*$), 338 ($n\rightarrow\pi^*$), 497 (d-d), 383 (L-M); MS: m/z: 741$[M+H]^+$;Λ_m(ohm^{-1} cm^2 mol^{-1}) 70.3; µeff (BM) 2.34.

Complex 3.

Bright yellow colour; yield: 57 %; M.P>300 °C; FTIR (ν cm^{-1}): 1635 (ν C=N), 1577 (ν C=C), 1395 (ν C-N), 1125 (ν N-N), 788(νM-N) and 530 (νM-NH); UV-vis. in DMSO, cm^{-1} (transition): 262, 298 ($\pi\rightarrow\pi^*$), 336 ($n\rightarrow\pi^*$) and 515, 733 (d-d); MS: m/z: 734$[M+H]^+$;Λ_m(ohm^{-1} cm^2 mol^{-1}) 88.9; µeff (BM) 5.46.

Complex 4.

Yellow colour; yield: 45 %; M.P>300 °C; FTIR (ν cm^{-1}): 1633 (ν C=N), 1577 (ν C=C), 1395 (ν C-N), 1130 (ν N-N), 500 (νM-N) and 493 (νM-NH); UV-vis. in DMSO, cm^{-1} (transition): 265, 299 ($\pi\rightarrow\pi^*$), 332 ($n\rightarrow\pi^*$) and 473 (d-d); MS: m/z: 742$[M+2H]^+$;Λ_m(ohm^{-1} cm^2 mol^{-1}) 87.4; µeff (BM) 3.56.

Complex 5.

Brown colour; yield: 60 %; M.P>300 °C; FTIR (ν cm^{-1}): 1635 (ν C=N), 1577 (ν C=C), 1398 (ν C-N), 1122 (ν N-N), 520 (νM-N) and 420(νM-NH); UV-vis. in DMSO, cm^{-1} (transition): 260, 295 ($\pi\rightarrow\pi^*$), 343 ($n\rightarrow\pi^*$),495, 520 (d-d) and 420 (L-M); MS: m/z: 727$[M^+]$;Λ_m(ohm^{-1} cm^2 mol^{-1}) 89.2; µeff (BM) 3.56.

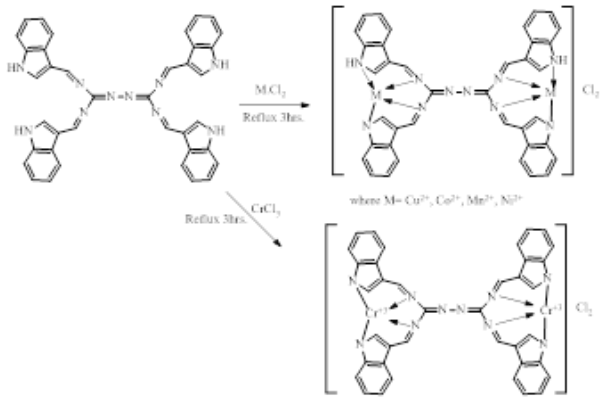

Figure 1. Proposed structure of the guanidine ligand metal complexes 1-5.

Biological activity

Maintenance of cell cultures

HCAM cell line was got from the Iraqi centre of cancer and continued in RPMI-1640 supplemented with 10% Fatal bovine, 100 units/mL penicillin, and 100 µg/mL streptomycin. cells were passaged by Trypsin-EDTA reseeded at 50% confluence twice a week and incubated at 37 °C and 5% $Co_2$was applied to humidify the atmosphere.

Combination Cytotoxicity Assays

The MTT (3-(4,5-dimethylthiazol-2-yl)-2,5-diphenyltetrazoliumbromide)cell viability assay was performed on 96-well plates, to determine the cytotoxic effect. The HCAM cell line was seeded at approximately 1 × 10^4 cells/well. After 24h or a confluent monolayer was performed, cells were treated with the prepared compounds using different concentrations (50, 250, 500, 750, 1000) µg/ml. Cell viability was recorded after 72 hours of treatment by removing the medium, adding 28 µL of 2 mg/mL solution of MTT and incubating the cells for 2 h at 37 °C. After removing the MTT solution, the crystals remaining in the wells were solubilized by the addition of 100 µL of dimethyl sulfoxide followed by 37 °C incubation for 15 min with shaking [16]. Absorbency was run on a microplate reader at 620 nm (test wavelength); the assay was reported in triplicate. The rate of inhibition for cell growth (the percentage of cytotoxicity) was considered as the following equation: Proliferation rate as (PR)= B/A*100 where A is the mean optical density of untreated wells and B is the optical density of treated wells and IR= 100- PR [17]. In addition to the concentration causing half the maximum inhibitory (IC50) was determined.

Result and discussion

The analytical and physical data (Table 1), spectral data (Tables 2 and 3) reveal that, the guanidine ligand (L) ($C_{38}H_{28}N_{10}$) was synthesized by condensation reaction of 1,2-hydrazinedicarboximidamide with Indol-3-carboxaldehyde in (1:4) molar ratio as shown in Scheme.1. The complexes 1-5 are designed in (1:2) (L: M) stoichiometric ratio (Fig.1). Based on the results of all the analytical studies, metal complexes 1-5 agreed to the proposed general formula of $[M_2L]$ Cl_2.

Conductivity

The high molar conductance values of the complexes (1-5) in DMF (10^{-3} M) invention in the 70.3-89.2 ohm^{-1} cm^2 mol^{-1} range as in Table 1,

representing that, all the complexes are an electrolyte [18]. This confirms that, the anion is not coordinated to the metal ion.

FT-IR spectra

The manners of bonding between the ligand and the metal ion can be exposed by comparing the IR spectra of the solid complexes (1-5) with that of the guanidine ligand (L). The IR spectral data of the ligand (Fig. 2a) and its metal complexes (Figs. 2b-f) are offered in Table 2. The IR spectrum of the ligand shows absorption band at 1672 cm^{-1} due to azomethine *ν* (CH=N) [19], a broad medium band appears at 3107 cm^{-1} assigned to the stretching vibration of the *ν* (N-H). The comparatively strong bands located at 1516, 1365 and 1132 cm^{-1} are assigned to the ν(C=C) $_{Ar}$, ν(C-N), ν(N-N) respectively. In all the metal complexes (1-5) indicated that the absorption band of azomethine group υ (CH=N) was shifted to lower frequencies in the range 1633-1637 cm^{-1} upon complexation with central metal ions, suggesting that the coordination happens via azomethine nitrogen [20]. Its packages weaken the υ (N-H) group, underscoring their association which appears in the ligand region 3107cm^{-1} disappears in the complexes. New vibrations at 500-788 cm^{-1} and 420-530 cm^{-1} which are not present in the free guanidine L are attributed to the existence of υ (M-N) and υ (M-NH).

Magnetic moments

The magnetic moments values of the complexes (1-5) lie in the 1.75-5.46 B.M as shown in Table (3). This strongly fever a distorted tetrahedral geometry around the metal ion and has para-magnetic properties [21].

Electronic spectra

The electronic spectral data for the guanidine ligand (L) and its metal complexes (1-5) in DMSO solution are summarized in Table (3). The ligand (Fig. 3a) in DMSO solution shows two bands at 357 nm (ε = 12880 $mol^{-1}cm^{-1}$) and 279 nm (ε = 2580 $mol^{-1}cm^{-1}$), which may be assigned to the n→π* and π→π* transitions respectively [22]. The bands appeared in the UV−vis spectra (Figs. 3b-f) of the complexes (1-5) in the 332-343 and 260-299 nm ranges were assigned to the ligand field (L.F). Thus, the band appeared in the 342-733 nm region indicated d →d transition in the complexes. The bands at 383 and 420 nm in the spectra of complexes 2 and 5 was due to the metal to ligand charge transfer transition (C.T) [23].

^{1}H, ^{13}C-NMR spectra for the guanidine ligand (L)

The ^{1}H-NMR spectrum for the ligand guanidine (L) in Fig.4 showed the following characteristic chemical shift (DMSO-d_6 as a solvent): the spectrum showed singlet signal at 11.51 ppm due to proton of NH group, and singlet signal at 8.92 ppm attributed to the azomethine proton (CH=N). As well as signals at 8.40-7.14 ppm range detected as multiple due to aromatic protons. The ^{13}CNMR spectrum of a ligand (L), Fig.5 in DMSO-d_6 solvent displayed that the chemical shift at 185.01ppm due to carbon of (CH=N) group, and the chemical shift at 155.11 ppm assigned to the carbon atom of (-C=N-N) group. While the chemical shift at 111.7-137.2 ppm range attributed to the aromatic carbons [24].

Mass Spectra for the guanidine ligand (L) and its complexes

The electrospray (ESI^+) mass spectra of ligand (L) and its metal complexes (1-5) exhibited successive fragments related to the structures. The parent ion peak for the ligand (Fig. 6a) observed at m/z 624 corresponding to M+ for $C_{38}H_{28}N_{10}$; requires 624.25. The other peak fragments were shown to give at m/z 118 (M+) for C_8H_8N, m/z 146 (M+) for $C_9H_{10}N_2$ and m/z 341 (M+) for $C_{20}H_{17}N_6$. Complex 1 (Fig. 6b) gave a molecular ion peak at m/z 750 which corresponds to M+ for $[Cu_2(C_{38}H_{28}N_{10})]$ Cl_2; requires 749.77. As well as the complex 2 (Fig. 6c) reveal a molecular ion peak at m/z 741 corresponding to $[M+H]^+$ for $[Co_2(C_{38}H_{29}N_{10})]$ Cl_2; requires 740.55. While the complex 3 (Fig. 6d) gave ion peak at m/z 734 which corresponds to $[M+H]^+$ for $[Mn_2(C_{38}H_{29}N_{10})]$ Cl_2; requires 732.56. The complex 4 (Fig. 6e) exhibited a molecular ion peak at m/z 742 corresponding to $[M+2H]^+$ for $[Ni_2(C_{38}H_{30}N_{10})]$ Cl_2; requires 740.07, and the complex 5 (Fig. 6f) gave ion peak at m/z 727 which corresponds to M+ for $[Cr_2(C_{38}H_{28}N_{10})]$ Cl_2; requires 726.67 [25].

Anticancer Activity

To examine the cytotoxic activity of the guanidine ligand (L) and its metal complexes (1-5), they were

tested for effects on the viability of the HCAM cell line using the 3-(4,5-dimethylthiazol-2-yl)-2,5-diphenyl tetrazolium bromide) (MTT) assay, and cisplatin is one of the most usually used anticancer drugs [26]. All of the complexes were tested from their low concentration (50 µg/ml) to higher concentration (1000 µg/ml). In vitro cytotoxic activity investigation revealed that complexes 1, 2 and 3 exhibited high activity with concentration of 50, 750 and 1000 µg/ml, and IC50 values of 87.73, 180 and 432 µg/ml, respectively. The results revealed that the cytotoxic activity of the Cu (II), Mn (II) and Co (II) complexes [27, 28] could be correlated with the donor atoms as (N_8)-type (Figs. 7-9). It is also important to note that the guanidine ligand (L) and complexes (4, and 5) did not show marked inhibition against the HCAM cancer cell line as shown in Table 4.

Table 1

Physical data of the ligand (L) and its metal complexes.

No.	Empirical formula	FW	Color	Yield (%)	M.P (°C)	Molar conductance Λm ($\Omega^{-1}cm^2mol^{-1}$)
L	$C_{38}H_{28}N_{10}$	624.71	yellow	75	255-258	-
1	$[Cu_2(C_{38}H_{26}N_{10})]\ Cl_2$	820.7	Pale brown	59	>300	77.6
2	$[Co_2(C_{38}H_{26}N_{10})]\ Cl_2$	811.5	Green	66	>300	70.3
3	$[Mn_2(C_{38}H_{26}N_{10})]\ Cl_2$	803.5	Bright yellow	57	>300	88.9
4	$[Ni_2(C_{38}H_{26}N_{10})]\ Cl_2$	811.0	yellow	45	>300	87.4
5	$[Cr_2(C_{38}H_{26}N_{10})]\ Cl_2$	797.6	Brown	60	>300	89.2

Table 2

IR frequencies of the bands (cm^{-1}) of ligand (L) and its metal complexes.

No.	ν (NH)	ν (CH=N)	ν $(C=C)_{Ar}$	ν (N-N)	ν (C-N)	ν (M-N)	ν (M-NH)
L	3107	1672	1516	1132	1365	---	---
1	---	1637	1521	1122	1444	640	486
2	---	1635	1562	1131	1446	532	430
3	---	1635	1577	1125	1395	788	530
4	---	1633	1577	1130	1446	500	493
5	---	1635	1577	1122	1398	520	420

Table 3

The electronic absorption spectral bands (nm) and magnetic moment (B.M) for the ligand (L) and its complexes

Compound	λ max (nm)	ε_{max} $mol^{-1}cm^{-1}$	Assignment	Suggested structure	µeff (B.M)

L	279 357	2580 12880	π→π* n→π*	-	-
1	262, 296 336 342	1183, 1193 441 20	L.F L.F $^3T_2 \rightarrow {}^3E$	tetrahedral	1.754
2	261, 298 338 383 497	1360, 1310 99 54 33	L.F L.F C.T $^4F A_2 \rightarrow {}^4P T_1$, $^4F A_2 \rightarrow {}^4T_1$, $^4F A_2 \rightarrow {}^4T_2$	tetrahedral	2.346
3	262, 298 336 515, 733	1180, 1930 441 19, 27	L.F L.F d-d	tetrahedral	5.468
4	265, 299 332 473	1160, 1450 154 10	L.F L.F $^3F T_1 \rightarrow {}^3P T_1$, $^3F T_1 \rightarrow {}^3A_2$, $^3F T_1 \rightarrow {}^3T_2$	tetrahedral	3.562
5	260, 295 343 420 495, 520	1700, 1670 130 35 44, 54	L.F L.F C.T $^4F A_2 \rightarrow {}^4P T_1$, $^4F A_2 \rightarrow {}^4T_2$	tetrahedral	3.562

Table 4
IC50 values for the ligand and its complexes against HCAM cell Line

Compound	Concentration µg/ml	IC50 µg/ml
L	-	-
1	50	87.73
2	1000	180
3	750	432
4	-	-
5	-	-

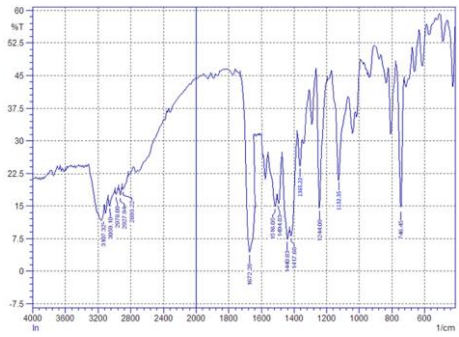

Fig. 2a. FT-IR spectrum of guanidine (L).

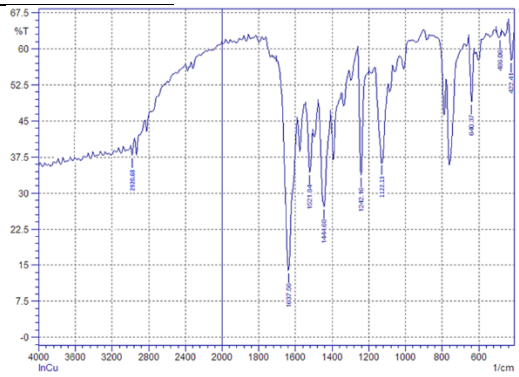

Fig. 2b. FT-IR spectrum of complex (1).

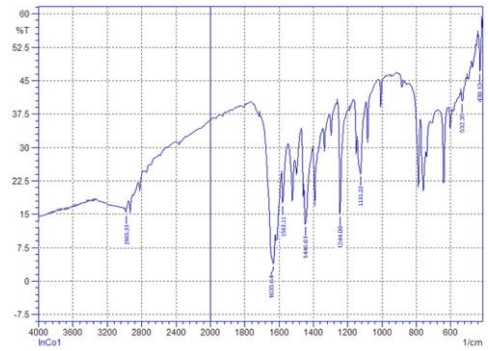

Fig. 2c. FT-IR spectrum of complex (2).

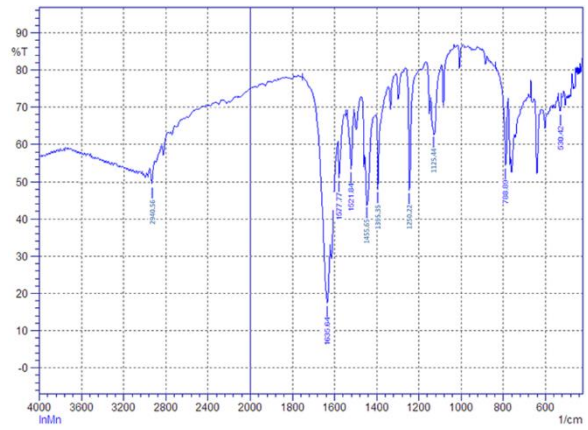

Fig. 2d. FT-IR spectrum of complex (3).

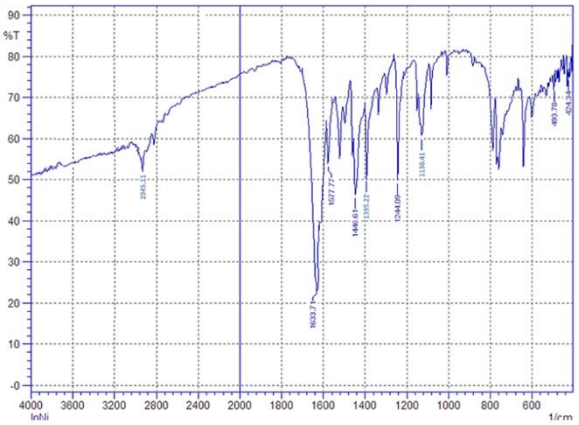

Fig. 2e. FT-IR spectrum of complex (4).

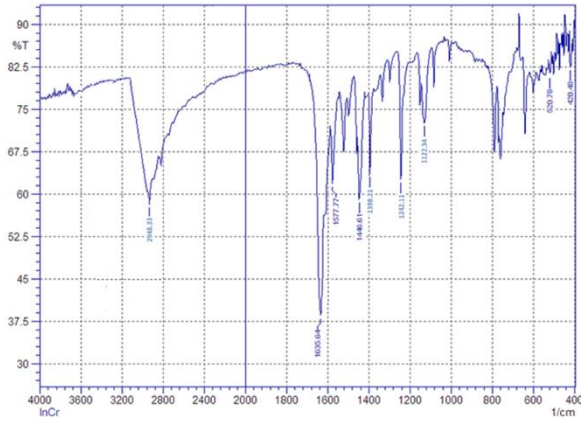

Fig. 2f. FT-IR spectrum of complex (5).

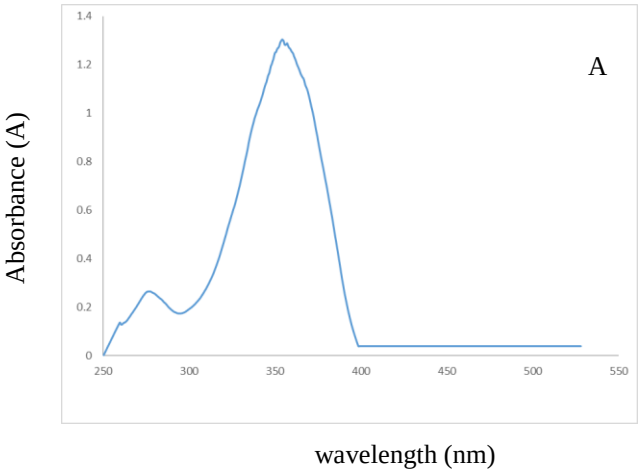

Fig. 3a. UV-Vis. spectrum of guanidine (L).

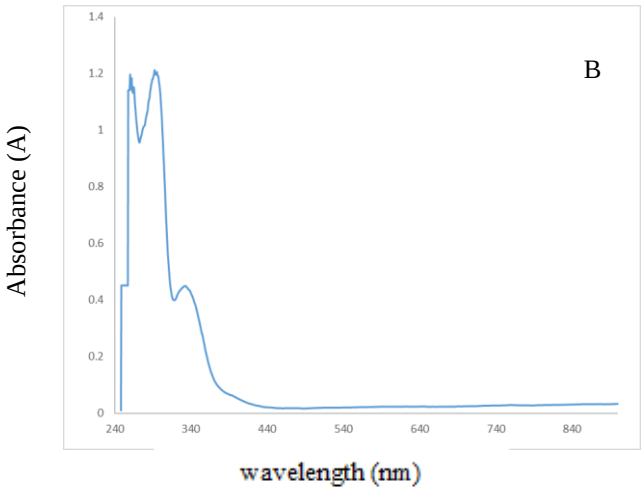

Fig. 3b. UV-Vis. spectrum of complex (1).

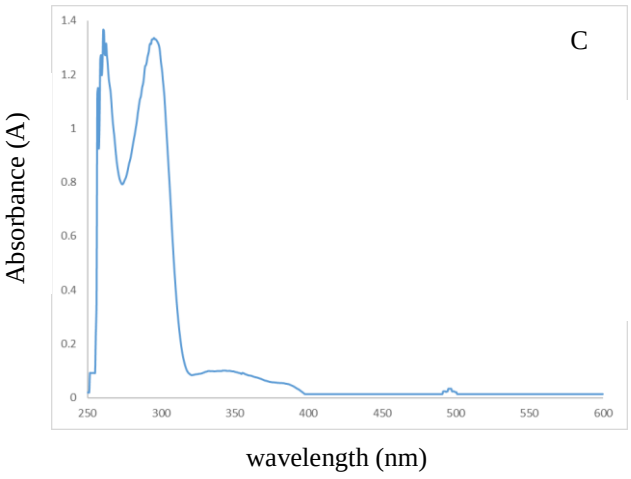

Fig. 3c. UV-Vis. spectrum of complex (2).

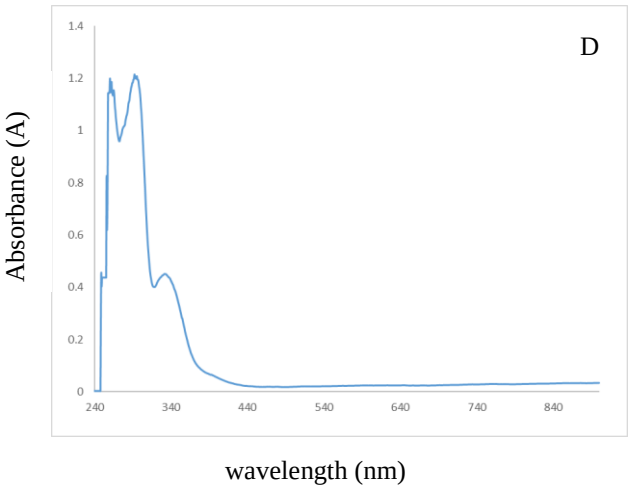

Fig. 3d. UV-Vis. spectrum of complex (3).

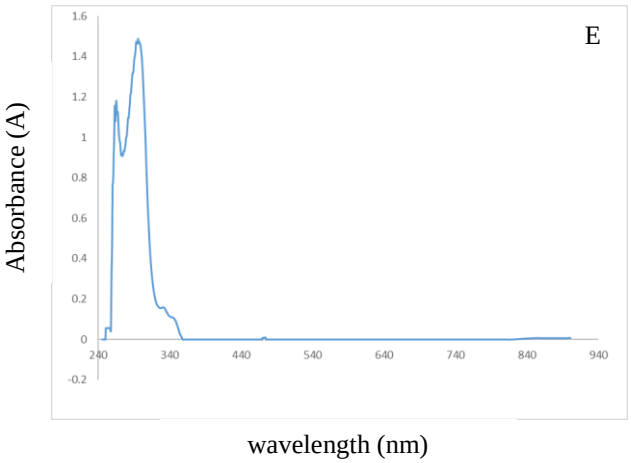

Fig. 3e. UV-Vis. spectrum of complex (4).

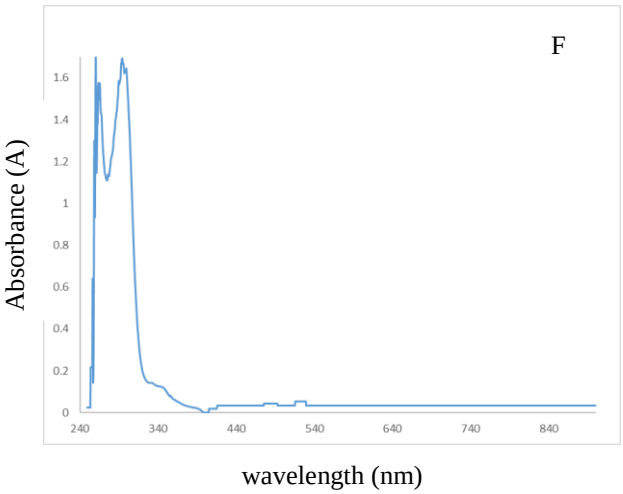

Fig. 3f. UV-Vis. spectrum of complex (5).

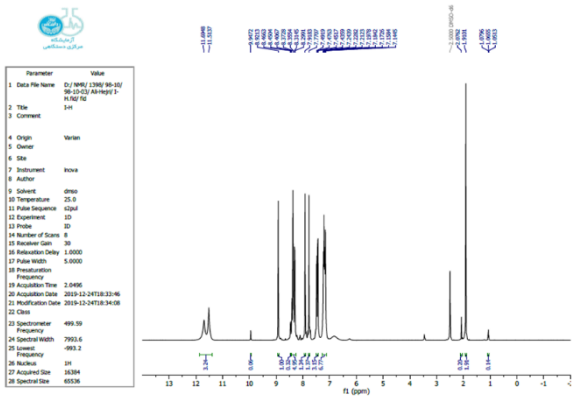

Fig. 4. ^{1}H NMR spectrum of guanidine (L).

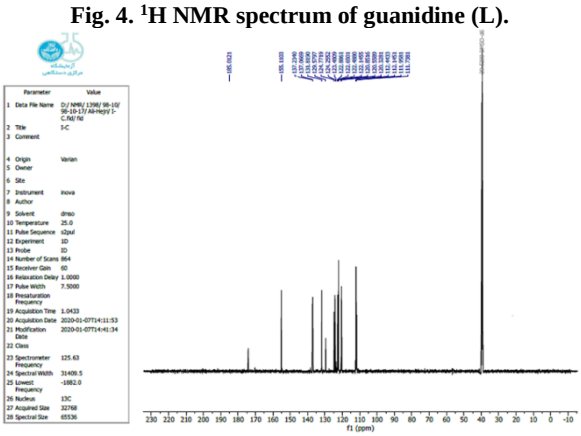

Fig. 5. ^{13}C NMR spectrum of guanidine (L).

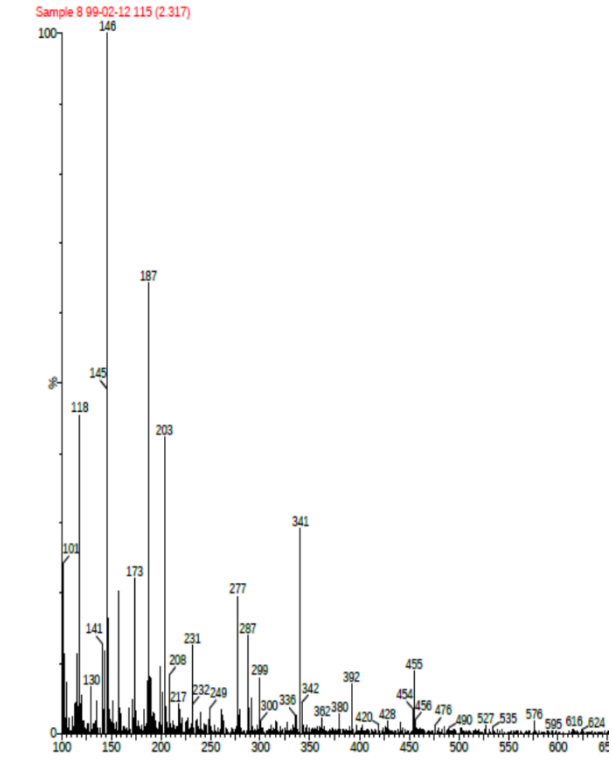

Fig. 6a. ESI-Mass spectrum of guanidine (L).

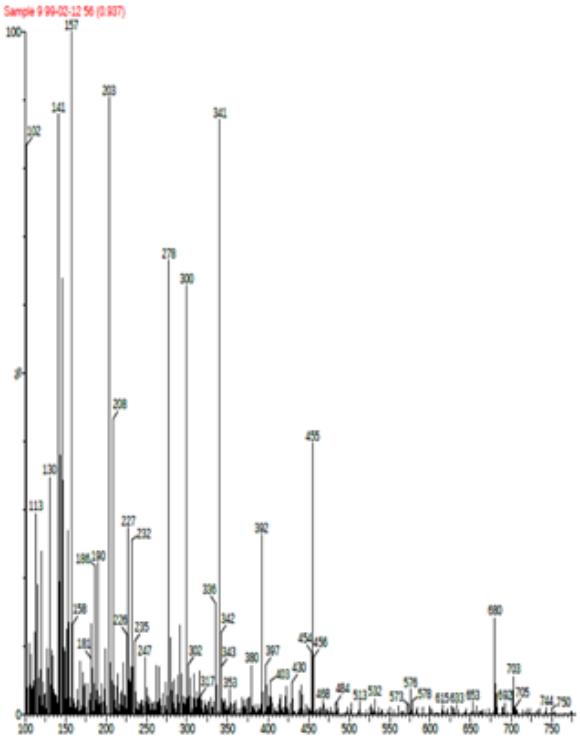

Fig. 6b. ESI-Mass spectrum of complex (1).

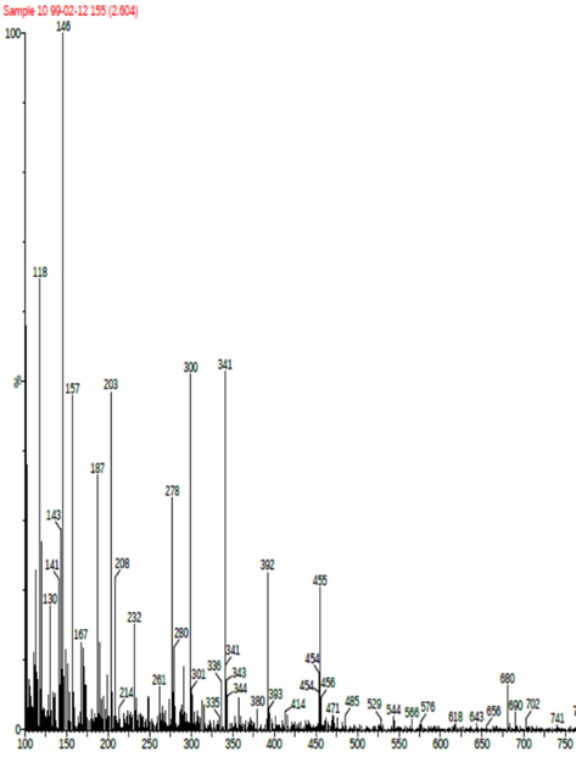

Fig. 6c. ESI-Mass spectrum of complex (2).

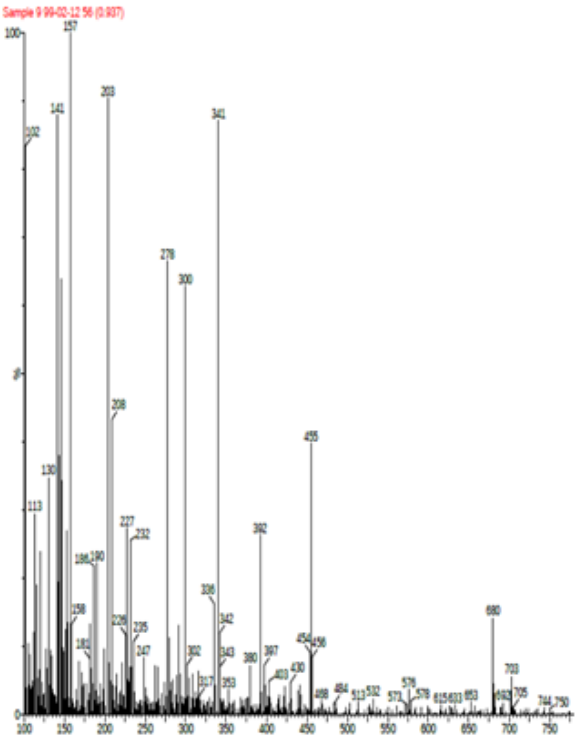

Fig. 6d. ESI-Mass spectrum of complex (3).

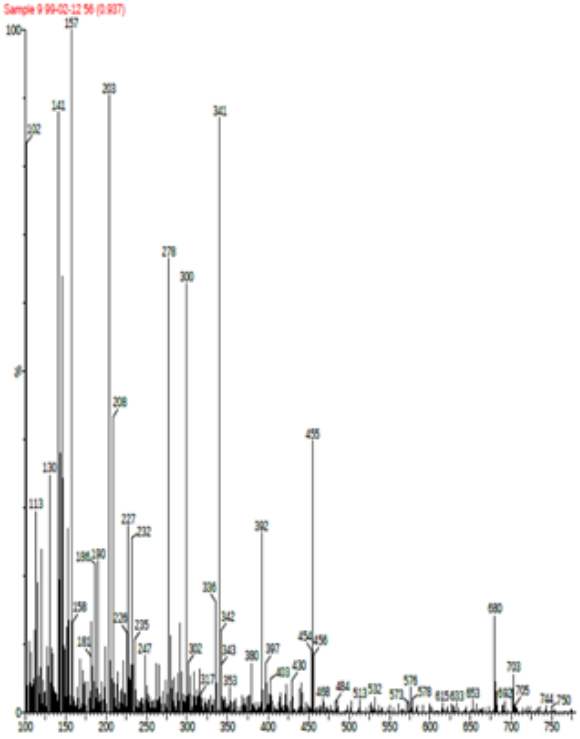

Fig. 6e. ESI-Mass spectrum of complex (4).

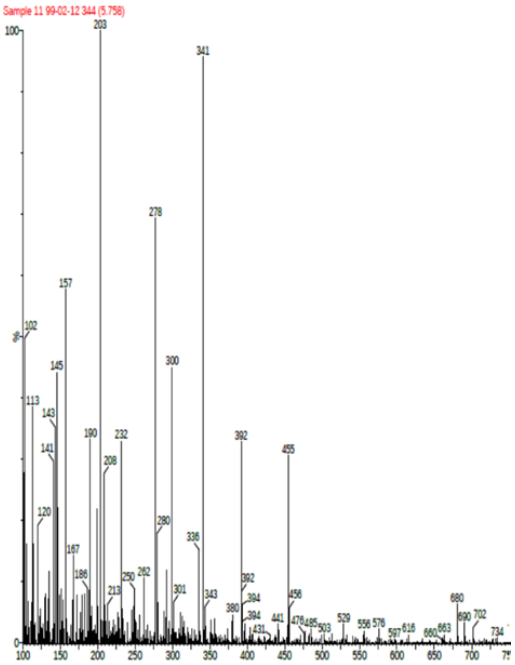

Fig. 6f. ESI-Mass spectrum of complex (5).

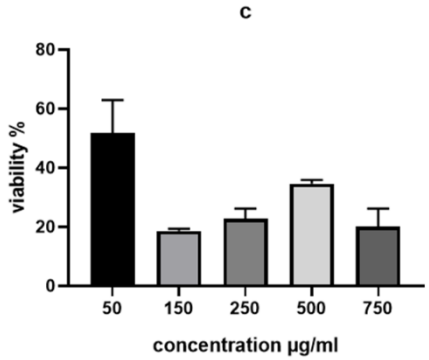

Fig. 7. Rate viability of HCAM cell line treated with five replicates of concentrations(µg/ml) from Cu (II) complex with IC50 in µg/ml.

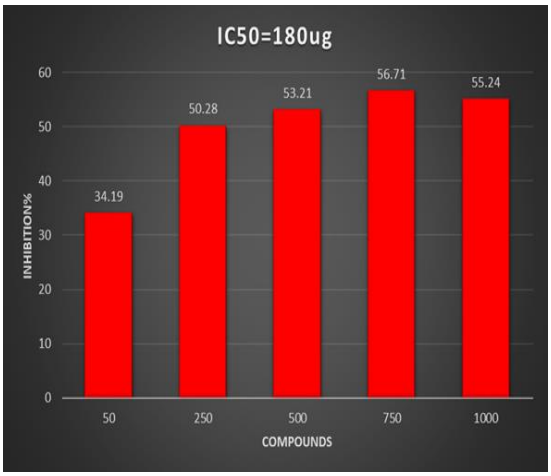

Fig. 8. Rate viability of HCAM cell line treated with five replicates of concentrations(µg/ml) from Co (II)) complex with IC50 in µg/ml.

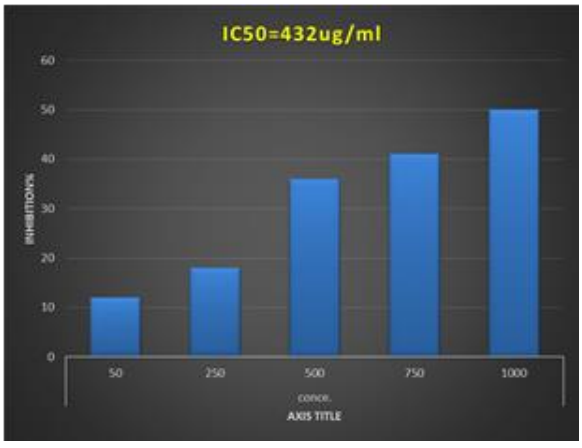

Fig. 9. Rate viability of HCAM cell line treated with five replicates of concentrations(µg/ml) from Mn (II)) complex with IC50 in µg/ml.

Conclusions

Five new metal complexes have been synthesized and described from binucleation ligand and well characterized through conventional analytical approaches and by various spectral physicochemical methods. The results of FTIR, electronic transition, ^{1}H and ^{13}C-NMR and mass spectrometry. In addition to the measurements of magnetic sensitivity and electric conductivity led to the conclusion that the metal complexes 1-5 assumed a distorted tetrahedral geometry. Among the five complexes, only Co (II) and Mn (II) complexes showed a good result against liver cancer cells, and they need further investigations to improve and identify the most active complex.

.

Conflicts of interest

There are no conflicts to declare

Acknowledgments

The authors express their sincere thanks to the Principal and the Management of Tissue Culture Lab. in College of Education for pure science in Basrah University. We extent our hearty thanks to the Management of the Iraqi Centre for Cancer and Medical Genetic Research.

REFERENCES

1. Berlinck, R.G.S., A.E. Trindade-Silva, and M.F.C. Santos, The chemistry and biology of organic guanidine derivatives. *Natural Product Reports*, 2012. **29**(12): p. 1382-1406.
2. Rawat, B.S., S.C. Mehra, and R. Tandon, SYNTHESIS AND ANTIMICROBIAL ACTIVITY OF SOME NEW HETEROCYCLIC GUANIDINE DERIVATIVES. *WORLD JOURNAL OF PHARMACY AND PHARMACEUTICAL SCIENCES*, 2016. **5**(9): p. 1325-1337.
3. Pingaew, R., N. Sinthupoom, P. Mandi, V. Prachayasittikul, R. Cherdtrakulkiat, S. Prachayasittikul, S. Ruchirawat, and V. Prachayasittikul, Synthesis, biological evaluation and in silico study of bis-thiourea derivatives as anticancer, antimalarial and antimicrobial agents. *Medicinal Chemistry Research*, 2017. **26**(12): p. 3136-3148.
4. Fuchs, M., S. Schmitz, P.M. Schäfer, T. Secker, A. Metz, A.N. Ksiazkiewicz, A. Pich, P. Kögerler, K.Y. Monakhov, and S. Herres-Pawlis, Mononuclear zinc(II) Schiff base complexes as catalysts for the ring-opening polymerization of lactide. *European Polymer Journal*, 2020. **122**: p. 109302.
5. Rittinghaus, R.D., P.M. Schäfer, P. Albrecht, C. Conrads, A. Hoffmann, A.N. Ksiazkiewicz, O. Bienemann, A. Pich, and S. Herres-Pawlis, Cover Feature: New Kids in Lactide Polymerization: Highly Active and Robust Iron Guanidine Complexes as Superior Catalysts (ChemSusChem 10/2019). *ChemSusChem*, 2019. **12**(10): p. 2037-2037.
6. Schäfer, P.M., P. McKeown, M. Fuchs, R.D. Rittinghaus, A. Hermann, J. Henkel, S. Seidel, C. Roitzheim, A.N. Ksiazkiewicz, A. Hoffmann, A. Pich, M.D. Jones, and S. Herres-Pawlis, Tuning a robust system: N,O zinc guanidine catalysts for the ROP of lactide. *Dalton Transactions*, 2019. **48**(18): p. 6071-6082.
7. Pasdar, H., B.H. Saghavaz, R. Khadivi, M. Davallo, and N. Foroughifar, synthesis and characterization of 2-(pyridin-2-yl)guanidine derivatives and their metal complexes as potential antibacterial agents using phosphoryl chloride. *International journal of pharmaceutical sciences and research*, 2019. **34**: p. 4304-4314.
8. Zhang, H.-J., X. Qin, K. Liu, D.-D. Zhu, X.-M. Wang, and H.-L. Zhu, Synthesis, antibacterial activities and molecular docking studies of Schiff bases derived from N-(2/4-benzaldehyde-amino) phenyl-N′-phenyl-thiourea. *Bioorganic & Medicinal Chemistry*, 2011. **19**(18): p. 5708-5715.
9. Rajasekar, M., S. Sreedaran, R. Prabu, V. Narayanan, R. Jegadeesh, N. Raaman, and A. Kalilur Rahiman, Synthesis, characterization, and antimicrobial activities of nickel(II) and copper(II) Schiff-base complexes. *Journal of Coordination Chemistry*, 2010. **63**(1): p. 136-146.
10. da Silva, C.M., D.L. da Silva, L.V. Modolo, R.B. Alves, M.A. de Resende, C.V.B. Martins, and Â. de Fátima, Schiff bases: A short review of their antimicrobial activities. *Journal of Advanced Research*, 2011. **2**(1): p. 1-8.
11. Deng, X. and M. Song, Synthesis, antibacterial and anticancer activity, and docking study of aminoguanidines containing an alkynyl moiety. *Journal of Enzyme Inhibition and Medicinal Chemistry*, 2020. **35**(1): p. 354-364.
12. Jevtovic, V., Anticancer Activity of Copper (II) Complexes with a Pyridoxal-Semicarbazone Ligand. *Research In Cancer and Tumor*, 2014. **3**(1): p. 1-5.
13. Hussain, A., M.F. AlAjmi, M.T. Rehman, S. Amir, F.M. Husain, A. Alsalme, M.A. Siddiqui, A.A. AlKhedhairy, and R.A. Khan, Copper(II) complexes as potential anticancer and Nonsteroidal anti-inflammatory agents: In vitro

and in vivo studies. *Scientific Reports*, 2019. **9**(1): p. 5237.
14. El-Tabl, A.S., J.J. Stephanos, M.M. Abd-Elwahed, E.E.-D. Metwally, and S.M. El-Gamasy, Synthesis, Structural Characterization and Cytotoxic Activity of Novel Symmetrical and Asymmetrical Metal Complexes of Guanidinium Schiff base. *Journal of Chemical, Biological and Physical Sciences*, 15. **5**(4): p. 3875-3907.
15. Hong, J., M. Cheng, Q. Liu, W. Han, Y. Zhang, Y. Ji, X. Jia, and Z. Li, Two cobalt(II) coordination polymers constructed from tetrafluoroterephthalate and hexamethylenetetramine ligands. *Transition Metal Chemistry*, 2013. **38**(4): p. 385-392.
16. Al-Shammari, A.M., M.I. Salman, Y.D. Saihood, N.Y. Yaseen, K. Raed, H.K. Shaker, A. Ahmed, and A. Khalid, In Vitro Synergistic Enhancement of Newcastle Disease Virus to 5-Fluorouracil Cytotoxicity against Tumor Cells. Biomedicines. *Biomedicines*, 2016. **4**(1): p. 3.
17. Freshney, R.I., Culture Vessels and Substrates, in *Culture of Animal Cells*. 2010, Copyright © 2010 John Wiley & Sons, Inc. p. 89-98.
18. Yousif, E.I., H.A. Hasan, R.M. Ahmed, and M.J. Al-Jeboori, Formation of macrocyclic complexes with bis(dithiocarbamate) ligand; synthesis, spectral characterisation and bacterial activity. *Der Chemica Sinica*, 2016. **7**(2): p. 53-65.
19. Kadhum, M.Y. and A.M. Abduljleel, Synthesis, characterization and biological studies of schiff bases derived from piperonal and their complexes with cobalt (II). *Der Pharma Chemica*, 2014. **6**(5): p. 88-100.
20. Meghdadi, S., M. Amirnasr, K. Mereiter, H. Molaee, and A. Amiri, Synthesis, structure and electrochemistry of Co(III) complexes with an unsymmetrical Schiff base ligand derived from 2-aminobenzylamine and pyrrole-2-carboxaldehyde. *Polyhedron*, 2011. **30**(10): p. 1651-1656.
21. Anacona, J. and J. Santaella, Synthesis, magnetic and spectroscopic studies of a Schiff base derived from cephaclor and 1,2-diaminobenzene and its transition metal complexes. *Spectrochimica Acta Part A: Molecular and Biomolecular Spectroscopy*, 2013. **115**: p. 800-804.
22. Mohammed, N.L., J.M.S. Al-Shawi, and M.J. Kadhim, Synthesis, Characterization and Thermal Studies of Schiff Bases Derived from 2,4-Dihydroxy benzaldehyde and their Complexes with Co(II), Ni (II), Cu(II). *International Journal of Scientific Engineering and Research*, 2019. **7**(1): p. 31-40.
23. Sonobe, T., T. Shimojima, A. Nakamura, M. Nakajima, S. Uchida, K. Kihou, C.H. Lee, A. Iyo, H. Eisaki, K. Ohgushi, and K. Ishizaka, Orbital-anisotropic electronic structure in the nonmagnetic state of BaFe2(As1−xPx)2 superconductors. *Scientific Reports*, 2018. **8**(1): p. 2169.
24. Gholizadeh Dogaheh, S., H. Khanmohammadi, and E.C. Sañudo, A new trinuclear N–N bridged Cu(II) complex with an asymmetric Schiff base ligand derived from hydrazine. *Polyhedron*, 2017. **133**: p. 48-53.
25. Tsednee, M., Y.-C. Huang, Y.-R. Chen, and K.-C. Yeh, Identification of metal species by ESI-MS/MS through release of free metals from the corresponding metal-ligand complexes. *Scientific Reports*, 2016. **6**(1): p. 26785.
26. Tokala, R., S. Bale, I.P. Janrao, A. Vennela, N.P. Kumar, K.R. Senwar, C. Godugu, and N. Shankaraiah, Synthesis of 1,2,4-triazole-linked urea/thiourea conjugates as cytotoxic and apoptosis inducing agents. *Bioorganic & Medicinal Chemistry Letters*, 2018. **28**(10): p. 1919-1924.
27. Parlak, A.E., Y. Karagozoglu, N.O. Alayunt, S. Turkoglu, I. Yildirim, M. Karatepe, and M. Koparir, Biochemical evaluation of hydroxyurea derivative schiff bases in liver of rats. *Cell Mol Biol (Noisy-le-grand)*, 2017. **63**(11): p. 5-10.
28. El-Tabl, A.S., M. Mohamed Abd El-Waheed, M.A. Wahba, and N. Abd El-Halim Abou El-Fadl, Synthesis, Characterization, and Anticancer Activity of New Metal Complexes Derived from 2-Hydroxy-3-(hydroxyimino)-4-oxopentan-2-ylidene)benzohydrazide. *Bioinorganic Chemistry and Applications*, 2015. **2015**: p. 126023.